

# Tension stiffening effect of RC panels subject to biaxial stresses

Hyo-Gyoung Kwak<sup>†</sup> and Do-Yeon Kim<sup>‡</sup>

Department of Civil and Environmental Engineering, KAIST,  
373-1 Guseong-dong, Yuseong-gu, Daejeon, 305-701, South Korea

**Abstract.** An analytical model which can simulate the post-cracking nonlinear behavior of reinforced concrete (RC) members such as bars and panels subject to uniaxial and biaxial stresses is presented. The proposed model includes the description of biaxial failure criteria and the average stress-strain relation of reinforcing steel. Based on strain distribution functions of steel and concrete after cracking, a criterion to consider the tension-stiffening effect is proposed using the concept of average stresses and strains. The validity of the introduced model is established by comparing the analytical predictions for reinforced concrete uniaxial tension members with results from experimental studies. In advance, correlation studies between analytical results and experimental data are also extended to RC panels subject to biaxial tensile stresses to verify the efficiency of the proposed model and to identify the significance of various effects on the response of biaxially loaded reinforced concrete panels.

**Keywords:** tension-stiffening; average stress-strain; reinforced concrete; biaxial tensile stresses.

---

## 1. Introduction

Since concrete is relatively weak and brittle under tension, cracking is expected when the significant tensile stress is induced in a member, and reinforcing steel is used to provide the necessary tensile strength for a structural member. Steel can be considered a homogeneous material and its material properties are generally well defined. On the other hand concrete is a heterogeneous material made up of cement, mortar and aggregates. Its mechanical properties scatter more widely and cannot be defined easily. For the convenience of analysis and design, however, concrete is often considered as a homogeneous material in the macroscopic sense.

Because of the low tensile strength of concrete, the nonlinear response of RC structures can be roughly divided into three ranges of behavior: (1) the uncracked elastic stage, (2) the crack propagation of concrete and (3) the plastic (yielding of steel or crushing of concrete) stage. The post-cracking behavior of RC structures also depends on many influencing factors (the tensile strength of concrete, anchorage length of embedded reinforcing bars, concrete cover, and steel spacing, etc.) which are deeply related to the bond characteristics between concrete and steel (*fib* 2000). Accordingly, to verify the nonlinear behavior of RC structures including the bond-slip mechanism, many experimental and numerical studies have been conducted in the past (Gupta and Maestrini 1990, Somayaji and Shah 1981, Yang and Chen 1988).

---

<sup>†</sup> Associate Professor

<sup>‡</sup> Post-Doctoral Researcher

In earlier studies, characterization itself of the tension stiffening effect due to the non-negligible contribution of cracked concrete was the main objective. Recently, following the introduction of nonlinear fracture mechanics in RC theory (Ouyang, *et al.* 1997, Barros, *et al.* 2001), more advanced analytical approaches have been conducted (Salem and Maekawa 1999, Sato and Vecchio 2003), and many numerical models which can implement the tension stiffening effect into the stress-strain relation of concrete have been proposed (Massicotte, *et al.* 1990, Gupta and Maestrini 1990, Belarbi and Hsu 1994). Christiansen and Nielsen (2001) presented a simple model for the prediction of plane stress behavior of reinforced concrete through determining stresses, strains and crack widths. Besides, the ACI committee 224 (1992) and CEB-FIP (1990) predict, in an empirical manner, the average stress-strain curves of a RC element subject to biaxial loadings.

Moreover, two basically different approaches have been used in defining the strain softening part in the tension region (ASCE 1982, CEB 1996, *fib* 2000): (1) a modified stiffness approach based on a repeated modification of stiffness according to the strain history; and (2) a bond-slip based model constructed from the force equilibrium and strain compatibility condition at the cracked concrete matrix with the assumed bond stress distribution. Even though the second approach is broadly adopted in finite element formulation, there are still some limitations in application because this approach requires the assumption of bond stress distribution function along the axis of reinforcement, and it follows a series of complex integration and derivation procedures to calculate the elongation and strain increment of steel and accompanying relative slip.

To address this limitation in adopting the bond-slip based tension stiffening model, an analytical approach to predict the post-cracking behavior of RC structures is introduced in this paper. Unlike previous approaches based on the assumed bond stress distribution function, the strain distribution of concrete, which is abruptly changed after cracking occurs, is defined with a polynomial function satisfying the boundary conditions at the crack face and at the inner end of the transfer length. The polynomial order is determined from the energy equilibrium condition before and after cracking. The validity of the introduced approach is established by comparing the analytical predictions for RC tension members with results from experimental and previous analytical studies. Moreover, numerical analyses for idealized RC panels are conducted to verify the applicability of the constructed tension stiffening model to RC containments subject to internal pressure.

## 2. Cracking behavior of tension member

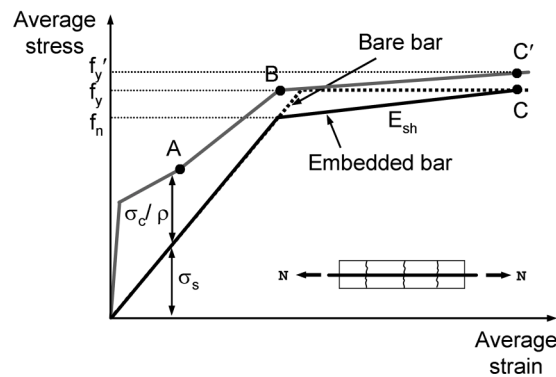
Tension stiffening effect can be illustrated by the relation between the average stress and the average strain of an axial member through the entire range from the uncracked state to the yielding state (see Fig. 1). During the formation of primary cracks, the average strains increase with a decrease of the stress in the concrete until a stabilized cracking state is reached (point A in Fig. 1). A continuous increase of loading results a gradual increase of the stiffness because of the bond resistance between concrete and steel, and the crack width is gradually enlarged without an additional change in the number of cracks up to the yielding of reinforcing steel at the crack (point B in Fig. 1). Moreover, when the average strain along the entire length of a member reaches the yielding strain, the stiffening effect of concrete ends at point C in Fig. 1.

Fig. 1, which illustrates the typical experimental responses of reinforcing steel, also shows that the average stress-strain curve of reinforcing bars embedded in concrete is very different from that of

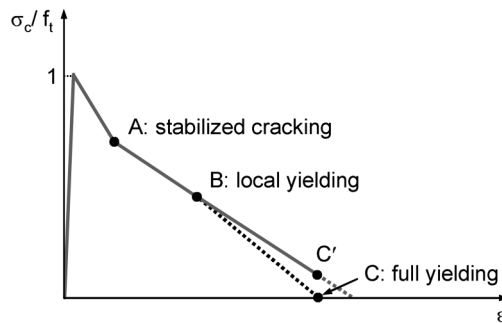
the bare steel bars. First, the average yield stress of embedded steel bars  $f_n$  is significantly less than the yield stress of bare steel bars  $f_y$  and, secondly, the post-yield range of the average stress-strain curve of RC composite represents a more inclined line, rather than an almost horizontal plateau in bare steel bars.

From these results mentioned above, the following can be inferred: (1) the tension stiffening model proposed in the CEB-FIP (1990), which assumes the same slope of the stress-strain relation with that of the bare steel bar on the basis of no bond-slip at the post-cracking stage (A-B region in Fig. 1) overestimates the stiffness of RC structure; and (2) a direct use of the stress-strain relation of bare steel bar will result in an overestimation of the post-yielding behavior of RC structures in the case of considering the tension stiffening effect into the stress-strain relation of concrete as shown in Fig. 1(b). (3) beyond steel yielding and up to the end of the yield plateau, the concrete matrix can contribute to the strength of a tension member through the remaining bond resistance (B-C' region in Fig. 1).

Accordingly, to trace the cracking behavior of RC structures up to the ultimate limit state by using the smeared crack model in which the local displacement discontinuities at cracks are distributed over some tributary area within the finite element and the behavior of cracked concrete is represented by average stress-strain relations (Kwak and Song 2002), the average stress-strain relation of steel needs to be defined. Considering these factors, the following average yield stress,



(a) Average stress-strain relation of RC tension member



(b) Average stress-strain relation of concrete

Fig. 1 Post-cracking behavior of RC tension member

which was introduced by Salem and Maekawa (1999) from the analytical results through correlation studies with experimental data, is used in this paper to revise the monotonic envelope curve of bare steel

$$f_n = f_y - \delta \frac{f_t}{\rho} \quad (1)$$

$$\delta = \frac{1}{\sqrt{1 + 1.5\rho f_y}} \quad (2)$$

### 3. Tension stiffening model of uniaxial tension member

#### 3.1. Bond-slip behavior of tension member

A part of an RC member subject to uniaxial tension is shown in Fig. 3. When the axial load  $N$  is applied, from the basic assumptions adopted, the far ends represent the fully cracked state with a steel strain of  $\varepsilon_{s2}$ . The tensile force  $N$  is transferred from the steel bar to the concrete by bond stress, and the value of the bond stress is zero at the inner end of the transfer length  $l_t$ . This means that there is no bond-slip within the central region of the transfer length. Moreover, it can be assumed that the strains in steel and concrete are equal to each other at  $x=l_t$ , and the strain value corresponds to  $\varepsilon_{s1}$ .

From the strain distribution, the local slip  $w(x)$  can be defined as the total difference in elongations between the reinforcement and the concrete matrix measured over the length between a distance  $x$  from a crack face and the center of the segment ( $x=s/2$ ). That is

$$w(x) = \int_x^{l_t} (\varepsilon_s(x) - \varepsilon_c(x)) dx \quad (3)$$

On the basis of the force equilibrium and the relation of Eq. (3), the very well-known following governing differential equation for the bond-slip can be obtained (Gupta and Maestrini 1990, *fib*

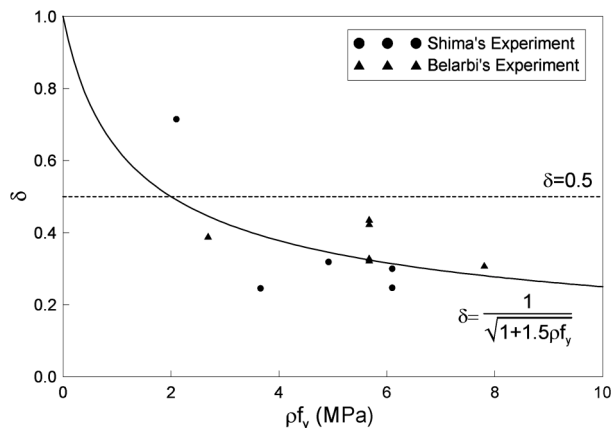


Fig. 2 Correction of coefficient  $\delta$

2000). The general solution of the differential equation is obtained in previous studies by applying the boundary conditions at the crack face and at the center of the cracked region based on an assumed bond stress distribution (Somayaji and Shah 1981, Yang and Chen 1988). However, this approach has some limitations in simulating the cracking behavior of RC axial members because it requires a series of complex integration and derivation procedures and the calculated location representing the maximum bond stress value is not coincident with that obtained from experimental study. To solve these limitations, an analytical approach on the basis of the assumed strain distribution function of concrete is introduced in this paper.

### 3.2. Determination of strain distributions

When the applied axial load  $N_1$  is relatively small, the strains in steel and concrete maintain a uniform distribution with  $\epsilon_{s1} = N_1 / (A_s E_s + A_c E_c)$  along the length. As the axial load ( $N_2$ ) gradually increases, the strains in steel and concrete represent different distributions in the region from the crack face to the inner end of the transfer length (see Fig. 4). Moreover, the steel strain  $\epsilon_{s2}$  at the crack face and  $\epsilon_{s1}$  at the center of the segment become  $\epsilon_{s2} = N_2 / (A_s E_s)$  and  $\epsilon_{s1} = N_2 / (A_s E_s + A_c E_c)$ , respectively.

From Fig. 4, the concrete strain distribution  $\epsilon_c(x)$  is assumed with a general  $n$ -th order polynomial function, and the steel strain distribution  $\epsilon_s(x)$  can also be expressed in terms of the concrete strain distribution function from the force equilibrium of  $N_2 = \epsilon_{s2} \cdot A_s E_s = \epsilon_{s1} \cdot (A_s E_s + A_c E_c)$  and the relation of  $\epsilon_{s1} = \epsilon_{c1}$ . The strain distributions lead to

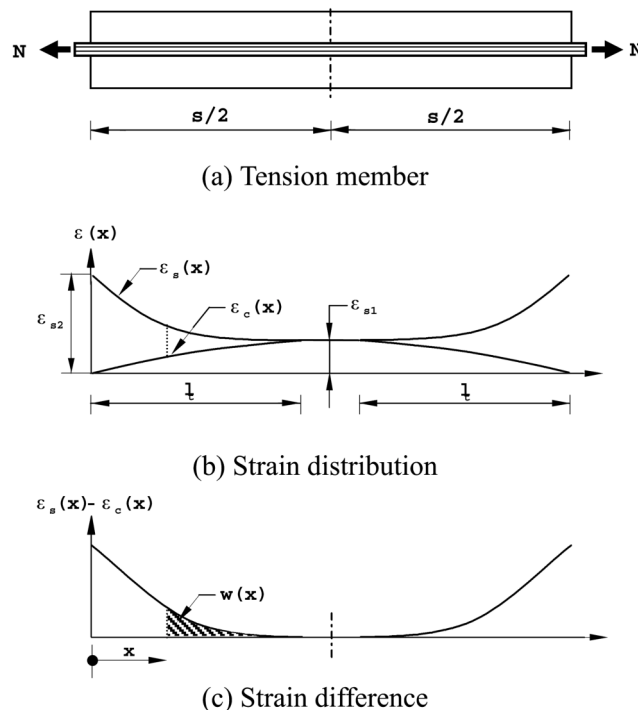


Fig. 3 Strain distribution in a part of an RC tension member

$$\epsilon_s(x) = \epsilon_{s2} - \frac{1}{n\rho} \epsilon_c(x) \tag{4a}$$

$$\epsilon_s(x) = \epsilon_{s1} \left\{ 1 - \left( 1 - \frac{x}{l_t} \right)^{n_c} \right\} \quad : x \leq l_t$$

$$\epsilon_s(x) = \epsilon_c(x) = \epsilon_{s1} \quad : l_t \leq x \leq s/2 \tag{4b}$$

where the area parameter  $n\rho$  is in the range of 0.02~0.5 (Gerstle, *et al.* 1978). Moreover, the transfer length  $l_t$  can be determined by the following linear relationship proposed by Somayaji and Shah (1981) on the basis of many experimental data for the pull-out tests.

$$l_t = K_p \frac{N_c}{\Sigma_o} \tag{5}$$

where  $N_c$  is the transfer load equal to  $N_c = A_c E_c \epsilon_{s1} = N / (1 + n\rho)$ , and  $K_p$  is a constant determined from the pull-out test. The experimental study by Houde and Mirza (1972) indicates that the value of  $K_p$  is in the range of 1/266~1/714 in<sup>2</sup>/lb, and the average value of 1/385 in<sup>2</sup>/lb is used in this paper.

The strain distribution of reinforcing bar changes from the uniform distribution  $\epsilon_{s1}$  along the segment before cracking to the assumed polynomial distribution with the strain  $\epsilon_{s2}$  at the crack face and  $\epsilon_{s1}$  at the inner end of the transfer length after cracking (see Fig. 4). From the energy conservation just before and after cracking at the same axial load  $N$ , the assumed polynomial order  $n_c$  can be determined because all the internal strain energy components can be represented in terms of the concrete strain with the assumed polynomial order  $n_c$ , while there is no additional external work by the axial load  $N$  at cracking. The strain difference of steel  $\epsilon_{s2} - \epsilon_{s1}$  means an increase of the strain energy at the reinforcing steel,  $\Delta U_s$ , and that of concrete  $\epsilon_{s1} - \epsilon_c(x)$  corresponds to a decrease of the strain energy at the concrete,  $\Delta U_c$ . Moreover, the difference between  $\Delta U_s$  and  $\Delta U_c$  means the energy loss caused by the bond-slip,  $U_b$ . Therefore, the energy conservation can be written as

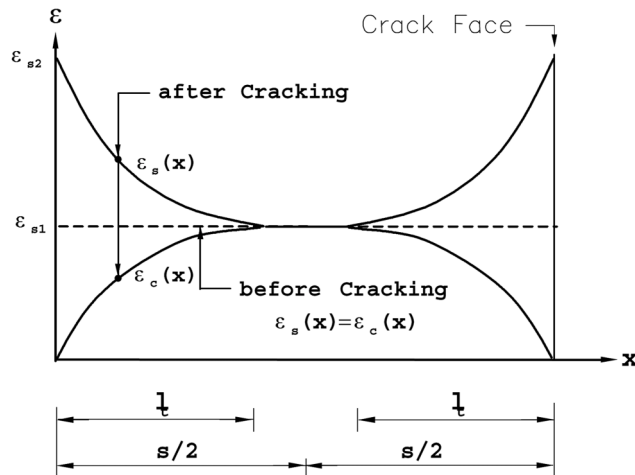


Fig. 4 Strain distribution after cracking

$$\Delta U_s - \Delta U_c = U_b \quad (6)$$

where

$$\Delta U_s = \int_V \Delta u_s dV = \int_V \int_{\varepsilon_{s1}}^{\varepsilon_s(x)} \sigma_s \circ \delta \, d\varepsilon dV = \frac{A_s E_s}{2} \int_0^l (\varepsilon_s(x)^2 - \varepsilon_{s1}^2) dx \quad (7a)$$

$$\Delta U_c = \int_V \Delta u_c dV = \frac{A_c E_c}{2} \int_0^l (\varepsilon_{s1}^2 - \varepsilon_c(x)^2) dx \quad (7b)$$

$$U_b = \sum_o \int_0^l \int_0^{w(x)} \tau_b(w(x)) dw dx \quad (7c)$$

and hence

$$\begin{aligned} \frac{A_c E_c}{2} \cdot \frac{\varepsilon_{s1} \varepsilon_{s2} l_t}{2n_c + 1} &= \frac{A_s E_s}{2} \cdot \frac{\varepsilon_{s1} \varepsilon_{s2} l_t}{n\rho(2n_c + 1)} \\ &= \frac{\sum_o \tau_{\max}}{w_1^a \cdot (1 + \alpha)} \times \frac{\varepsilon_{s2}^{1+\alpha} \cdot l_t^{1+\alpha} \cdot l_t}{(n_c + 1)^{1+\alpha} \cdot ((n_c + 1)(1 + a) + 1)} \end{aligned} \quad (8)$$

While calculating the bond energy variation  $U_b$ , the relation of Eq. (3) and the following nonlinear bond stress-slip relation (CEB-FIP 1990) are used.

$$\tau_b = \tau_{\max} \cdot (w(x)/w_1)^\alpha \quad (9)$$

where  $\tau_{\max}$  is the maximum bond stress of concrete, and  $w_1$  and  $\alpha$  have the values of 1 mm and 0.4, respectively, when a very good bonding condition is maintained in a confined concrete (CEB-FIP 1990).

As shown in Eqs. (7a)-(7c), all the strain energy variations are expressed with the assumed polynomial order  $n_c$ . Consequently, the order  $n_c$  can be determined through the successive iteration using the bisection method until Eq. (8) is satisfied.

### 3.3. Average stress-strain relation of concrete

If the applied axial load  $N$  in a tension member reaches to 1.3 times  $N_{cr}$  at the first crack, the specimen shows the stabilized crack pattern without additional occurrence of cracking (CEB-FIP 1990, FIB 1999), and the strain distribution along the member length can be represented by Fig. 5 (CEB-FIP 1990). After the crack formation has finished (point A in Fig. 1), the maximum crack spacing between adjacent cracks can be assumed to be 2.0 times the minimum crack spacing and is equal to the transmission length  $l_t$  (length over which slip between steel and concrete occurs) (CEB-FIP 1990).

From the geometric configuration for the strain distribution in Fig. 5, the average strain of reinforcing steel can be expressed as

$$\varepsilon_{sm} = \left( 1 - \frac{3}{4} \frac{n_c}{n_c + 1} \frac{1}{1 + n\rho} \right) \frac{\sigma_{s2}}{E_s} \quad (10)$$

where  $\sigma_{s2}$  is the steel stress at the crack face when the applied axial load has  $N = 1.3N_{cr}$  and can be calculated as

$$\frac{\sigma_{s2}}{f_t} = 1.3 \cdot \frac{1 + n\rho}{\rho} \quad (11)$$

As shown in Fig. 5, on the other hand, the strain distribution of concrete decreases in contrast to an increase of the steel strain because of a decrease of the bond resistance and represents the concrete strain itself not considering the crack width (Belarbi and Hsu 1994). Accordingly, to satisfy the assumption for the consistent displacement field between concrete and steel, the strain increment developed from the consideration of the crack width needs to be added. It might be reasonable to assume that the average concrete strain  $\epsilon_{cm}$  at the stabilized crack condition can be simulated by the average steel strain  $\epsilon_{sm}$  defined in Eq. (10). With the average strain determined and the force equilibrium equation, the average stress of concrete at the stabilized crack condition can also be calculated as follows

$$\sigma_c = \frac{\sigma_{s2}A_s - \epsilon E_s A_s}{A_c} \quad (12)$$

From the CEB-FIP (1990), the coefficient  $\alpha$  in Eq. (9) lies between 0 and 1. As the value of  $n_c$  increases according to an increase in  $\alpha$ , the minimum value of  $n_c$  can be assumed as 1.0. The tension stiffening effect corresponding to an arbitrary applied axial load  $N_m$  can be defined with the strain difference between  $\epsilon_{s2}$  and  $\epsilon_{sm}$  ( $\epsilon_{TS} = \epsilon_{s2} - \epsilon_{sm}$ ). Moreover, the average steel strain can be represented by  $\epsilon_{sm} = \epsilon_{s2} - 1/n\rho \cdot \epsilon_{cm}$  from Eq. (4a), and the average concrete strain can also be expressed by  $\epsilon_{cm} = n_c/(n_c+1) \cdot \epsilon_{s1}$  within the transfer length range when the strain distribution of  $\epsilon_{cm}(x)$  is defined with a  $n_c$ -th polynomial function. Accordingly, the strain difference corresponding to the tension stiffening effect can finally be expressed by  $\epsilon_{TS} = \epsilon_{s2} - \epsilon_{sm} = 1/n\rho \cdot \epsilon_{cm}$ . From this, the strain difference at the crack formation stage and that at the crack stabilizing stage are  $\epsilon_{TS}^{cr} = 1/n\rho \cdot n_c^{cr}/(n_c^{cr}+1) \cdot \epsilon_{s1}$  and  $\epsilon_{TS}^{st} = 0.75/n\rho \cdot n_c^{st}/(n_c^{st}+1) \cdot \epsilon_{s1}$ , respectively. On the other hand, the strain difference  $\epsilon_{TS}$  must be gradually decreased as the applied axial load  $N$  increases. Namely, the strain difference at the first cracking ( $\epsilon_{TS}^{cr}$ ) must always be greater than that at the stabilized cracking ( $\epsilon_{TS}^{st}$ ), and this condition induces the following inequality condition of

$$0.75 \cdot \left( \frac{n_c^{st}}{n_c^{st} + 1} \right) \leq \left( \frac{n_c^{cr}}{n_c^{cr} + 1} \right) \cdot \frac{\epsilon_{s1}^{cr}}{\epsilon_{s1}^{st}} \quad (13)$$

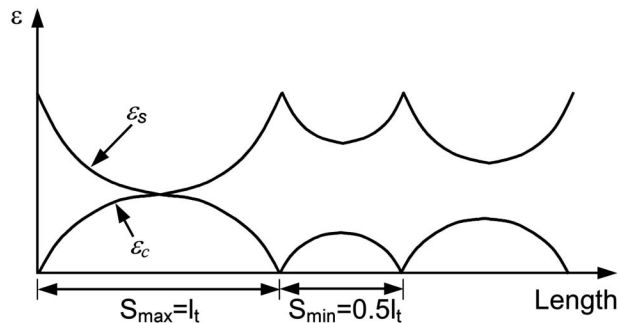


Fig. 5 Stabilized crack pattern with  $S_{max} = 2S_{min}$  (CEB-FIP 1990)

Consequently, the successive iteration of Eq. (8) must be continued in the range of  $n_c$  which satisfies Eq. (13). From Eqs. (8) and (13),  $n_c^{st}$  should increase by about 10% more than  $n_c^{cr}$  for generally used reinforcement ratio. Hence, it can be assumed  $n_c^{st} \approx n_c^{cr}$ .

A continuous increase of the axial load  $N$  over the stabilized cracking load leads to the yielding of reinforcing steel at the crack face while maintaining the elastic state at the other region (point B in Fig. 1). It means that the average steel stress of the embedded steel bar through the entire length will be smaller than that of the bare steel bar. A portion of the resisting capacity corresponding to the difference of yielding stress between the bare steel bar and the embedded steel bar must be carried by concrete. Therefore, the effective concrete stress  $\sigma_c$  and strain  $\varepsilon_c$  at point B in Fig. 1(b) can be calculated by

$$\frac{\sigma_c}{f_t} = (f_y - f_n) \frac{\rho}{f_t}, \quad \varepsilon = \frac{f_n}{E_s} \quad (14)$$

More increase of the axial load  $N$  finally cause the yielding of the embedded steel bar along the entire span length. To study the influence that bar yielding and large strains have on tension stiffening, a series of RC prisms were tested by Mayer and Eligehausen (1998). As a result, the yield plateau of the bare steel bar practically disappears in the member response, since the plastic strains in the embedded steel bar are limited to the regions close to the main cracks and hardly contribute to the overall elongation. Namely, a larger axial load corresponding to the yielding of the bare steel bar can still be resisted in the post-yielding range of steel. On the other hand, the post-yield behavior of RC members was described as the ratio ( $\varepsilon_{sm}/\varepsilon_{sr}$ ) between the average steel strain esm and the steel strain  $\varepsilon_{sr}$  at the crack face with respect to  $\varepsilon_{sr}$ , as shown in Fig. 6.

As long as the concrete is uncracked, the ratio  $\varepsilon_{sm}/\varepsilon_{sr}$  should be equal to 1. After abrupt drop of the ratio  $\varepsilon_{sm}/\varepsilon_{sr}$  at the first cracking because of a local increase of steel strain at the crack face, it should increase again between first cracking and bar yielding. Beyond  $\varepsilon_y$ , and up to the end of the yield plateau, the ratio esm/esr significantly reduces, until hardening is activated ( $\varepsilon_{sr} = \varepsilon_{sh}$ ). The step reduction is caused by the build-up of the plastic strain  $\varepsilon_{sr}$  close to the bending cracks, while the strains between the cracks are still elastic and exhibit high gradients. It means that the concrete contributes to the strength of a tension member even after yielding of steel through the remaining bond resistance.

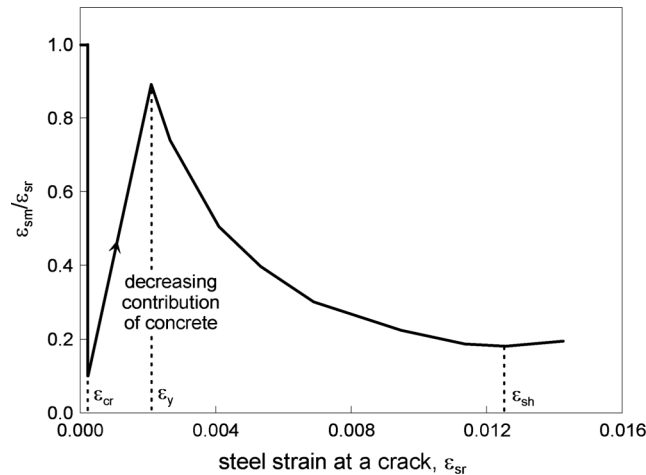


Fig. 6 Relation between esm and esr at post-yielding stage

To take into account this contribution of concrete at the post-yielding stage, the slope of the average stress-strain relation is changed in this paper. As shown in Figs. 1(a) and 1(b), the slope of line BC,  $\rho E_{sh} = \rho(f_y - f_n) / (\epsilon_{sh} - \epsilon_{sm})$ , have been modified to the slope of line BC',  $\rho(E_{sh} - (f_y' - f_n) / (\epsilon_{sh} - \epsilon_{sm}))$ , where the stress differences  $f_y - f_n$  and  $f_y' - f_y$  can be assumed to be 0.89 and 0.18, corresponding to  $\epsilon_{sr} = \epsilon_{sy}$  and  $\epsilon_{sr} = \epsilon_{sh}$  in Fig. 6, respectively. The slope of line BC' seems to be converged to  $0.8\rho E_{sh}$  instead of  $1.0\rho E_{sh}$ , and the average stress-strain relation of concrete in the region BC' is followed with the equilibrium equation.

#### 4. Extension of model to biaxial stresses

Unlike the reinforcing bars embedded in the concrete element, whose biaxial material properties are assumed to be simulated by the direct superposition of each element without any change in material properties, concrete under combinations of biaxial stress exhibits different strength and stress-strain behaviors from those under uniaxial loading conditions by the effects of Poisson's ratio and microcrack confinement. To simulate the change of material properties according to the biaxial tensile stress state, it is required to define the biaxial strength envelope in the tension-tension region.

Fig. 7 shows the biaxial strength envelope of concrete under biaxial tension. In contrast to a shear wall which experiences a biaxial stress combination in the tension-compression region, most of wall in the containment structures subject to internal pressure experiences biaxial stress combinations in the tension-tension region. Accordingly, in the biaxial strength envelope in the tension-tension region is regarded to be of great importance. In this paper, the biaxial strength envelope proposed by Aoyagi and Yamada (1983) is used, and the accompanying equation for the failure envelope in the tension-tension region is expressed by

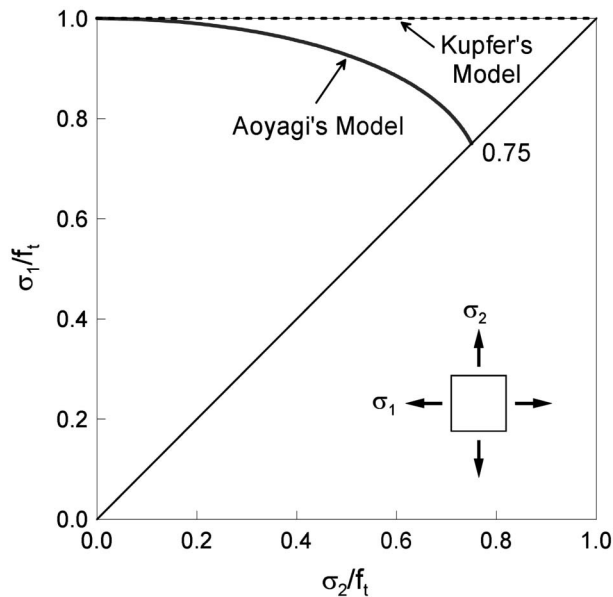


Fig. 7 Biaxial strength envelope of concrete under biaxial tension

$$\frac{\sigma_{1p}}{f_t} = 1 - 0.25 \left( \frac{\sigma_2}{\sigma_1} \right)^2 \quad (15)$$

The tensile strength in the primary direction decreases with increasing tensile stress in the other principal stress direction, and the failure takes place basically by cracking in the primary direction. When the cracking occurs, however, the principal tensile stress and strain in the other direction still remain in the ascending branch of the concrete stress-strain relation. Therefore, the proposed model introduced in this paper follows the assumption that the concrete stress-strain relation in the other direction ( $\sigma_2$  direction in Fig. 7) is the same as that of uniaxial loading and does not change with the variation of tensile stress in the primary direction before concrete cracking. Using the tensile strength  $\sigma_{1p}$  determined from Eq. (15), the stress-strain relation of concrete in the tension part can finally defined on the basis of the uniaxial tension stiffening model introduced in this paper (see Fig. 1).

In addition to the definition for the constitutive relations of concrete under biaxial loadings, additional modifications for the stress-strain relation of steel is also required. From the biaxial loading test for a series of orthogonally reinforced concrete panels, Pang and Hsu (1995) found that there was a substantial difference in the apparent yield stress  $f_n$  between 90 deg panels with the longitudinal steel oriented at 90 deg to the applied principal stress and 45 deg panels with the longitudinal steel oriented at 45 deg. As shown in Fig. 8, the apparent yield stresses  $f_n$  for 45 deg panels are lower than those for 90 deg panels by approximately 12 percent, regardless of the parameter  $B = (f_t/f_y)^{1.5}/\rho$  derived by Belarbi and Hsu (1994), and this reduction is attributed to the kinking of steel bars at the cracks.

When this 12% reduction is applied to the equation of  $f_n/f_y = 0.43 + 0.5f_y^*/f_y$ , introduced by Belarbi and Hsu (1994), it results the average yield strength reduction of about  $0.06f_y$ . In addition, Yamada's experimental results (Yamada and Aoyagi 1983) also show that the maximum shear strength of RC panels occurs at 45 deg panels because of the most dominant dowel action and its magnitude symmetrically decreases up to the angle of 90 deg between the longitudinal steel and the applied principal stress.

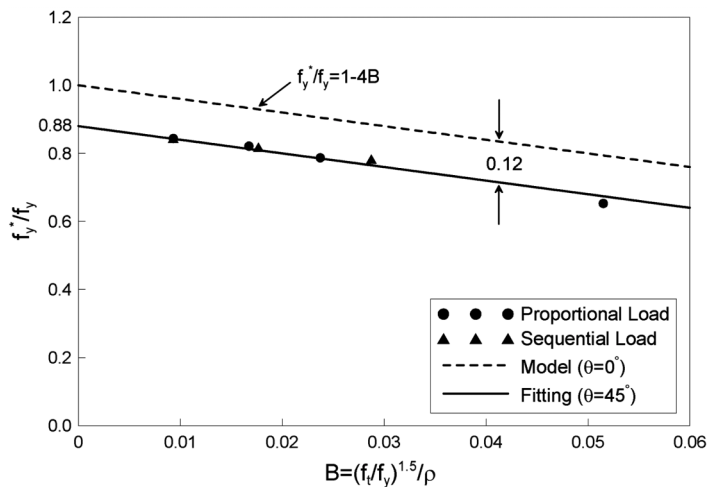


Fig. 8 Apparent yield stress of steel bars as function of parameter B

Accordingly, to define the average stress-strain relation of steel embedded in concrete panels with an arbitrary angle  $\theta$  to the applied principal stress, Eq. (1) defined for the uniaxial behavior of RC axial member has been modified as follows:

$$f_n = f_y - \delta \frac{f_t}{\rho} - 0.06f_y \sqrt{\frac{|\theta|}{45}} \quad -45 \leq \theta \leq 45 \quad (16a)$$

$$f_n = f_y - \delta \frac{f_t}{\rho} - 0.06f_y \sqrt{\frac{90-|\theta|}{45}} \quad \begin{array}{l} 45 \leq \theta \leq 90 \\ -90 \leq \theta \leq -45 \end{array} \quad (16b)$$

On the other hand, an exact assessment of the cracking in RC panels subject to general membrane stresses seems to be very difficult because of many influencing factors such as different steel ratios in both directions and changing crack angles according to the stress ratios. Most constitutive models to trace the cracking behavior of concrete, therefore, are based on the material matrix in the principal axes, using the equivalent steel ratio of  $\rho_{eq}f_y = \rho_x f_y \cos^2 \theta + \rho_y f_y \sin^2 \theta$  (Massicotte, *et al.* 1990) derived from the force equilibrium equation at the fully cracked ultimate state of a RC panel. This approach can be effectively used in concrete panels orthogonally reinforced with similar steel ratios in both directions but also has some limitations in application to other RC panels.

When the steel ratios in both directions represent a remarkable difference, the reinforcement with a smaller steel ratio will govern the tension stiffening effect, and in advance, the post-cracking behavior of RC panels. Accordingly, for an exact simulation of the cracking behavior, it might be proper to calculate the tensile stress and strain of concrete along the steel direction first, instead of the principal directions of concrete. Then, these stress and strain are transformed into the principal directions of concrete by

$$\varepsilon_{c1} = \varepsilon_x \cos^2 \theta + \varepsilon_y \sin^2 \theta + \gamma_{xy} \cos \theta \sin \theta \quad (17a)$$

$$\sigma_{c1} = \sum \sigma_{ci} \cos^2(\theta - \alpha_i) \quad (17b)$$

where  $\theta$  is the angle between the direction normal to the crack and the global  $x$ -axis, and  $\alpha_i$  is the orientation of reinforcement relative to the global  $x$ -axis.

## 5. Numerical applications

To study the behavior of reinforced concrete structures subject to biaxial tension, such as containment walls of nuclear power plants, a comparison of analytical predictions with experimental results from panels tested in the Korea Atomic Energy Research Institute (KAERI) (Chung 2000) was carried out. Among the tested panels, panels designated as S40, S60, R2 and R3 were selectively analyzed in this paper.

The specimen dimensions were 1500 mm  $\times$  1500 mm  $\times$  600 mm for S40 and S60, 1000 mm  $\times$  1000 mm  $\times$  380 mm for R2, and 900 mm  $\times$  900 mm  $\times$  380 mm for R3. Reinforcement was arranged at 90 deg, with respect to the applied loading directions ( $x$ ,  $y$  coordinates in Fig. 10). The loading ratio and material properties of each panel are summarized in Table 1. Specimens were subject to biaxial tension in the  $x$ ,  $y$ -directions.

Panels are modeled with a single four-node element because of the uniformity of the strain and



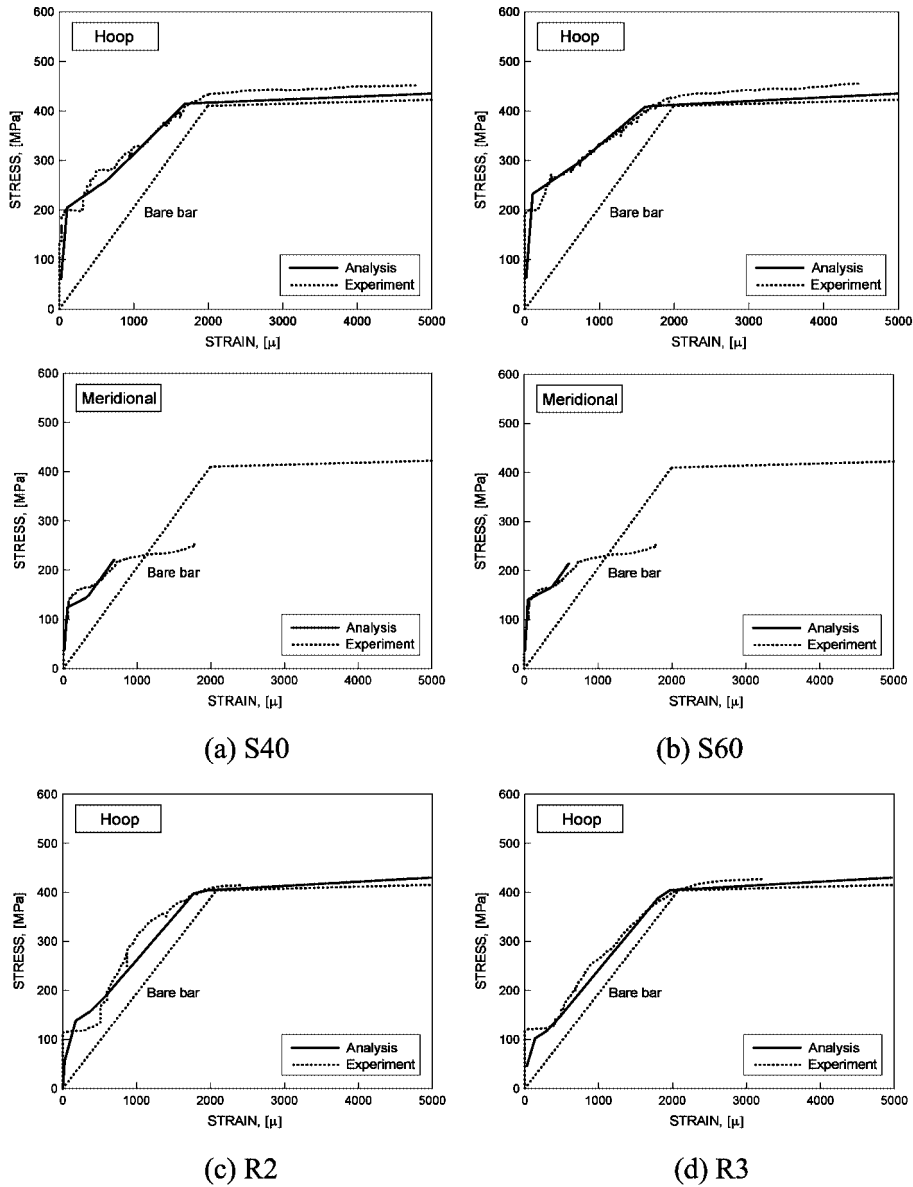


Fig. 10 Average stress-strain curves of biaxial tension specimens

$n$ -th order polynomial function is assumed and the polynomial order is determined on the basis of the energy equilibrium before and after cracking. The effective concrete stress-strain relation at the yielding state is derived from the average steel stress of the embedded steel bar. By adopting the proposed model, the post-cracking behavior of RC tension member can be easily analyzed without any additional complex calculation. The efficiency and reliability of the proposed model is demonstrated through application examples of biaxially loaded RC panels.

## Acknowledgements

The research reported in this paper was made possible by the financial support from the Smart Infra-Structure Technology Center funded by the Korea Science and Engineering Foundation. The authors would like to express their gratitude to this organization for the financial support.

## References

- ACI Committee 224. (1992), "Cracking of concrete members in direct tension", *ACI 224.2R-92*, American Concrete Institute, Detroit.
- Aoyagi, Y., and Yamada, K. (1983), "Strength and deformation characteristics of reinforced concrete shell elements subjected to in-plane forces", *Proc. JSCE*, **331**, 167-180.
- ASCE Task Committee on Finite Element Analysis of Reinforced Concrete Structures. (1982), *State-of-the-Art Report on Finite Element Analysis of Reinforced Concrete*, ASCE, New York.
- Barros M. H. F. M., Martins R. A. F., and Ferreira, C. C. (2001), "Tension stiffening model with increasing damage for reinforced concrete", *Engineering Computations*, **18**(5-6), 759-785.
- Belarbi, A., and Hsu, T. T. C. (1994), "Constitutive laws of concrete in tension and reinforcing bars stiffened by concrete", *ACI Struct. J.*, **91**(4), 465-474.
- CEB. (1996), *RC Elements under Cyclic Loading: State of the Art Report*, Thomas Telford Services Ltd., London.
- Christiansen, M. B., and Nielsen, M. P. (2001), "Plane stress tension stiffening effects in reinforced concrete", *Magazine of Conc. Res.*, **53**(6), 357-365.
- Chung, W. K. (2000), "Prestressed concrete containment structural element test", *KAERI CM-420*, Korea Atomic Energy Research Institute, Daejeon.
- Comité Euro-International du Béton. (1993), *CEB-FIP model code 1990*, Thomas Telford Service Ltd., London.
- FIB. (2000), *Bond of Reinforcement in Concrete*, State-of-Art Report Prepared by Task Group Bond Models, International Federation for Structural Concrete (*fib*), Lausanne.
- FIB. (1999), *Structural Concrete: Textbook on Behavior, Design and Performance*, Bulletin No. 1, FIB, Switzerland.
- Gerstle, W., Ingraffera, A. R., and Gergely, P. (1978), "Tension stiffening: a fracture mechanics approach", *Bond in Concrete*, Applied Science Publishers, London.
- Gupta, A. K., Mastrini, S. R. (1990), "Tension-stiffness model for reinforced concrete bars", *J. Struct. Eng., ASCE*, **116**(3), 769-790.
- Houde, J., and Mirza, M. S. (1972), "A study of bond stress-slip relationship in reinforced concrete", *Struct. Conc. Series No. 72-8*, McGill University, Montreal, Quebec.
- Kwak, H. G., and Song, J. Y. (2002), "Cracking analysis of RC members using polynomial strain distribution function", *Eng. Struct.*, **24**(4), 455-468.
- Massicotte, B., Elwi, A. E., and MacGregor, J. G. (1990), "Tension-stiffening model for planar reinforced concrete members", *J. Struct. Eng., ASCE*, **116**(11), 3039-3058.
- Mayer, U., and Eligehausen, R. (1998), "Bond behavior of ribbed bars at inelastic steel strains", *Proc. 2<sup>nd</sup> Int. Ph. D. Symposium in Civil Engineering*, Technical Univ. of Budapest, Hungary, 39-46.
- Ouyang, C., Wollrab, E., Kulkarni, S. M., and Shah, S. P. (1997), "Prediction of cracking response of reinforced concrete tensile members", *J. Struct. Eng., ASCE*, **123**(1), 70-78.
- Pang, X. B., and Hsu, T. T. C. (1995), "Behavior of reinforced concrete membrane elements in shear", *ACI Struct. J.*, **92**(6), 665-679.
- Salem, H., and Maekawa, K. (1999), "Spatially averaged tensile mechanics for cracked concrete and reinforcement in highly inelastic range", *Concrete Library of JSCE*, **34**, 151-169.
- Sato, Y., and Vecchio, F. J. (2003), "Tension stiffening and crack formation in reinforced concrete members with fiber-reinforced polymer sheets", *J. Struct. Eng., ASCE*, **129**(6), 717-724.
- Shima, H., Chou, L., and Okamura, H. (1987), "Micro and macro models for bond in RC", *J. The Faculty of Engineering*, University of Tokyo (B), **39**(2), 133-194.

- Somayaji, S., and Shah, S. P. (1981), "Bond stress versus slip relationship and cracking response of tension members", *ACI Struct. J.*, **91**(4), 465-474.
- Yamada, K., and Aoyagi, Y. (1983), "Shear transfer across cracks", *Proc. JCI 2<sup>nd</sup> Colloquium on Shear Analysis of RC Structures*, JCI, 19-28.
- Yang, S., and Chen, J. (1988), "Bond slip and crack width calculation of tension members", *ACI Struct. J.*, **85**(7), 414-422.

CC